Effect of Aggregate Microtexture Losses on Skid Resistance: Laboratory-Based Assessment on Chip Seals

Basri Ergin[1]; İslam Gökalp[2]; and Volkan Emre Uz[3]

Abstract: Skid resistance has long been recognized as one of the most important pavement surface characteristics for safer roads. Evaluation of skid resistance of pavement is crucial but it is not an easy task. Moreover, it depends on numerous parameters such as pavement type, materials and tire properties, and environmental conditions. Aggregate texture changes significantly according to its origin and affects the skid resistance performance of the road surfaces. In the current study, chip seal samples were produced with different aggregate types at different polishing levels to evaluate the effect of aggregate microtexture on skid resistance performance. The Micro-Deval (MD) test device was utilized to obtain polished aggregates. Different polishing levels were provided by distinct revolutions of the MD drum. To monitor the change in aggregate surface with the polishing process, aggregates were monitored by scanning electron and optical microscopes at each level. Mean texture depths (MTDs) of chip seals were determined with outflow meter test. On the other hand, dynamic friction tester (DFT) and British pendulum tester (BPT) were implemented for assessment of skid resistance according to the relevant ASTM standards. Skid resistance and texture measurements were further used to identify the International Friction Index (IFI) for each sample. In addition, a correlational analysis was conducted between DFT and BPT results, and variable relationships were set for different speeds. Consequently, better skid resistance values were observed for chip seals produced by slags than the ones with natural aggregates at each polishing level. After fulfilling the economic and environmental requirements, using metallurgical by-products is recommended for long-lasting skid-resistant pavement surfaces. Additionally, it can be concluded that MD apparatus may be considered an easier, more cost-effective, and faster way to assess the polishing resistance of aggregates. **DOI: [10.1061/(ASCE)MT.1943-5533.0003096](https://doi.org/10.1061/(ASCE)MT.1943-5533.0003096).** © *2020 American Society of Civil Engineers.*

Author keywords: Skid resistance; Surface texture; Dynamic friction tester (DFT); British pendulum tester (BPT); Micro-Deval (MD); Chip seal; Slags.

Introduction

In Turkey, than one million traffic accidents occurred in the year 2017, and 0.2 million of them resulted in deaths or injuries (TUIK 2017). Several studies showed that the causes of road accidents are human, road, vehicle, and environmental factors or combinations of these. Although human-related accidents are more dominant than the others, the rate of accidents caused by road defects should not be underestimated (Karlaftis and Golias 2002; Mayora and Piña 2009).

The surface of the pavement may be deteriorated with time due to traffic loadings, environmental conditions, and poor maintenance/ rehabilitation management (Sarsam and Al Shareef 2015; Wang et al. 2015b). Loss of skid resistance of a pavement surface, a major cause of vehicle skidding especially on wet surfaces, is the significant reason for road condition-related traffic accidents. Skid resistance is the force developed when the tire is prevented from rotating along the surface, and its importance can be seen from previous studies that highlighted that a decrease in skid resistance leads to an increase in traffic accidents (Do and Cerezo 2015; Kane et al. 2013; Kogbara et al. 2018; Mataei et al. 2016; Nataadmadja et al. 2015; Uz and Gökalp 2017b). However, the progression level of skid resistance mainly depends on factors such as the type of pavement, properties of the pavement materials, and traffic levels (Wang et al. 2017).

Skid resistance of pavement has been affected by its surface texture during service life (Ansari et al. 2000; Black and Jackson 2000). Pavement surface texture is categorized into four main classes based on the texture amplitude and wavelength: microtexture, macrotexture, megatexture, and unevenness or roughness. As a function of aggregate mineralogy, microtexture ensures direct tire-pavement contact and interaction with traffic and climate factors. The macrotexture provides quick drainage of water over the pavement surface due to the hysteresis component of the friction. Megatexture describes irregularities of the road surface that may be revealed from pavement distress including rutting, potholes, patching, and cracks, and it is responsible for noise levels and rolling resistance of the pavement. The final texture, unevenness or roughness, may be revealed by construction errors and it affects ride quality and vehicle operating costs (Cossale et al. 2013; Do and Cerezo 2015; McLean 1995; Praticò and Vaiana 2015; Sengoz et al. 2012; Uz and Gökalp 2017a).

Numerous methods have been developed to assess the surface texture and skid resistance of pavements. These methods can be grouped as portable/vehicle-mounted and static/dynamic, based on their operating and measuring principles, respectively. Sand patch and outflow meter tests (OFM) are the portable methods based on volumetric measurements of the pavement surface texture depth, while circular texture meter and vehicle-mounted laser profilometer

[1]Civil Engineer, Dept. of Purchasing, Adana Metropolitan Municipality, Atatürk St., Adana 01120, Turkey. Email: basrirergin@hotmail.com

[2]Research Assistant and Ph.D. Candidate, Faculty of Engineering, Dept. of Civil Engineering, AAT Science and Technology Univ., Adana 01250, Turkey (corresponding author). Email: islamgokalp@gmail.com

[3]Associate Professor, Faculty of Engineering, Dept. of Civil Engineering, Izmir Institute of Technology, Izmir 35430, Turkey. Email: vemreuz@gmail.com

© ASCE   04020040-1   J. Mater. Civ. Eng.

J. Mater. Civ. Eng., 2020, 32(4): 04020040

are used to evaluate the mean profile depth of a road section (Flintsch et al. 2003). Dynamic friction tester (DFT), British pendulum tester (BPT), and locked-wheel skid resistance tester (LWSRT) are different skid resistance measurement methods based on different operating principles (Saito et al. 1996). The International Friction Index (IFI) was developed by PIARC-World Association to harmonize different test methods and classify friction properties of different pavement surfaces (PIARC 1987).

Pavements are exposed to challenging environmental conditions and repetitive traffic loads during their service life. The characteristics of materials used are an important task in building skid-resistant road pavements. It is known that skid resistance of a road surface is directly affected with aggregate and binder properties. Here, the resistance of an aggregate against polishing is a key feature and needs to be evaluated in an accurate way (Gökalp and Uz 2017). Various devices and methods have been developed and utilized for examining the polishing resistance of aggregates. Some of the common ones are polish stone value, Aachen polishing

machine, Wehner/Schulze machine, Auckland pavement polishing, Road test machine, and Micro-Deval (MD) test apparatus (Cafiso and Taormina 2007; Do et al. 2009; Friel and Woodward 2013; Kane et al. 2013; Wang et al. 2013). The standard or modified version of MD test method used in the current study was utilized by many researchers (Crouch and Goodwin 1995; Mahmoud and Masad 2007; Ortiz and Mahmoud 2014; Xue et al. 2010) to assess polishing resistance of different aggregates under different polishing agents and test durations. Moreover, polishing levels of aggregates were visually assessed by advance methods such as scanning electron microscope (SEM), optical polarized microscopy (OPM), and aggregate imaging systems (AIMS) before and after the tests.

Considering the scarce resources of natural aggregates, it is vitally important to create sustainable transportation infrastructures network and to use the aggregate resources effectively (El-Assaly and Ellis 2001; Gökalp et al. 2018; Kua 2015; Ossa et al. 2016; Plank 2008; Prezzi et al. 2011). In this regard, reducing the consumption of raw material and increasing the use of alternative

Table 1. Physical and mechanical properties of the aggregates

Order	Tests	Methods	Units	Results					Limitations[a]
				LS	BS	BLD	EAF	FER	
1	Abrasion resistance	EN 1097-1	%	11.7	9.4	11.3	9.5	7.6	≤25
2	Fragmentation resistance	EN 1097-2	%	24.4	25.9	17.5	22.9	16.5	≤30
3	Weathering resistance	EN 1367-2	%	8.1	9.4	6.2	2.3	6.1	≤18
4	Polishing resistance	EN 1097-8	PSV	41.6	52.4	57.9	76.1	61.7	≥40
5	Dry unit weight	EN 1097-6	g/cm^3	2.69	2.67	2.73	3.40	2.93	—
6	Water absorption	EN 1097-6	%	0.28	1.44	0.90	1.79	1.10	≤2.5
7	Flakiness index	EN 933	%	15.9	23.8	17.9	8.1	10.4	≤20
8	Friable particle values	ASTM C 142	%	0.81	0.63	0.41	0.23	0.23	0.3

Note: LS = limestone; BS = basalt; BLD = river basin crushed aggregate; EAF = electric arc furnace steel slag; and FER = ferrochromium slag.
[a]Limit values in Turkish Highway Technical Specification.

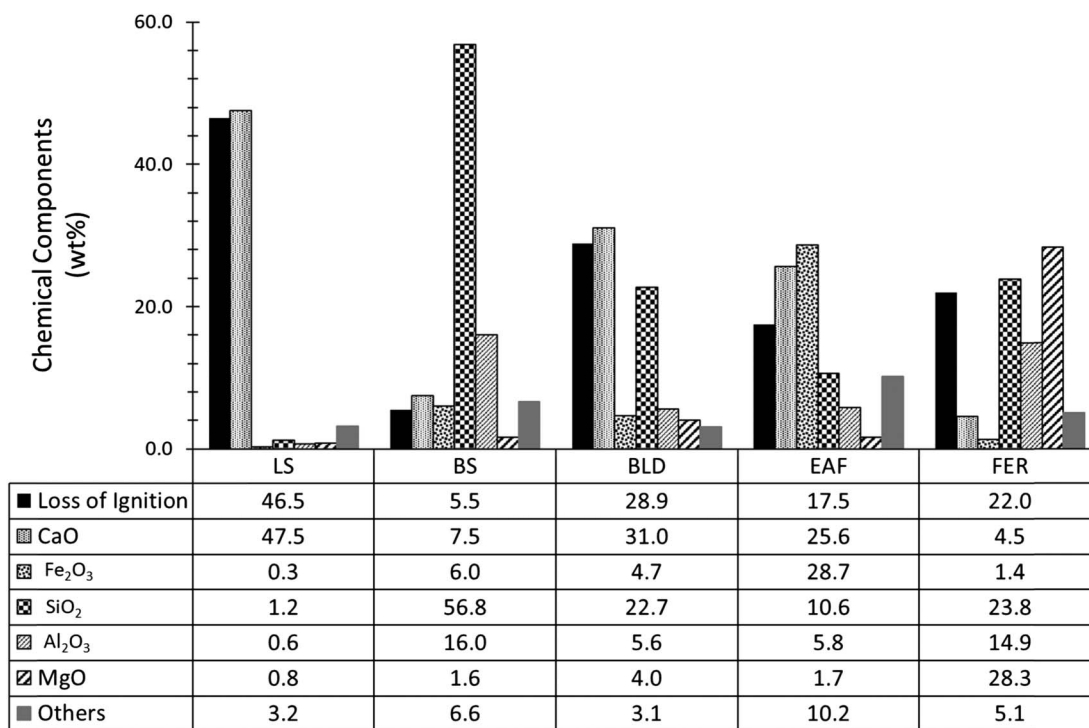|	LS	BS	BLD	EAF	FER
■ Loss of Ignition	46.5	5.5	28.9	17.5	22.0
▦ CaO	47.5	7.5	31.0	25.6	4.5
▨ Fe_2O_3	0.3	6.0	4.7	28.7	1.4
▨ SiO_2	1.2	56.8	22.7	10.6	23.8
▨ Al_2O_3	0.6	16.0	5.6	5.8	14.9
▨ MgO	0.8	1.6	4.0	1.7	28.3
■ Others	3.2	6.6	3.1	10.2	5.1

Fig. 1. Results of XRF analyses. LS = limestone; BS = basalt; BLD = river basin crushed aggregate; EAF = electric arc furnace steel slag; and FER = ferrochromium slag.
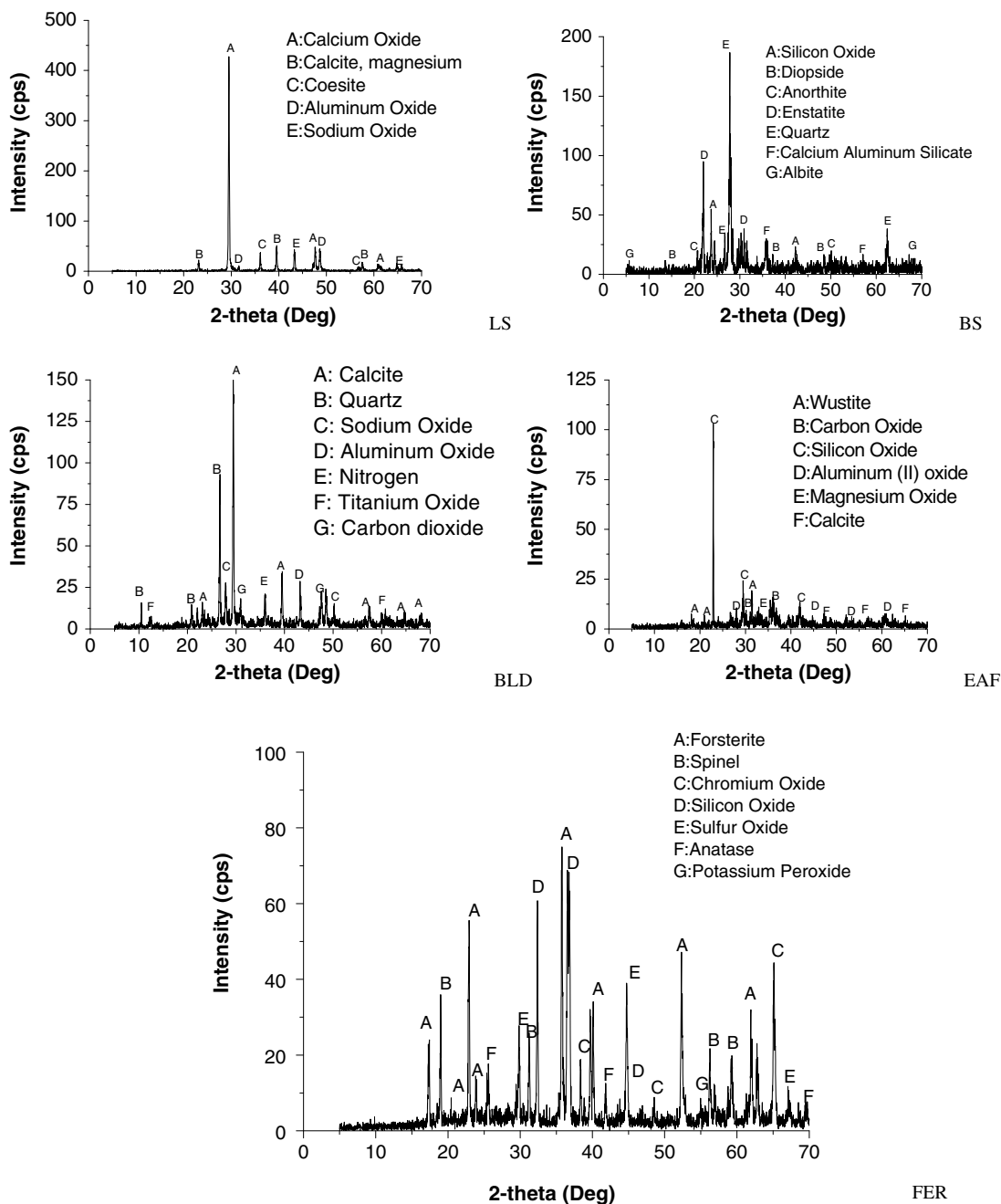
Fig. 2. Results of XRD analyses. LS = limestone; BS = basalt; BLD = river basin crushed aggregate; EAF = electric arc furnace steel slag; and FER = ferrochromium slag.

materials (waste/by-products) in highway construction has long been an area of interest for sustainable transportation. The objective of these efforts is to substitute natural aggregates with alternative materials without sacrificing structure performance. Numerous studies (Bessa et al. 2014; Chaurand et al. 2007; Gökalp et al. 2018; Kehagia 2009; Krayushkina et al. 2012; Xirouchakis and Manolakou 2011; Ziari and Khabiri 2007) have investigated the physical and chemical characteristics of metallurgical slags and their influence on the environment. Results of these studies showed that technical features of slags meet the relevant material specifications and slags were specified as inert or nonhazardous materials.

In Turkey, more than 1,000 quarries are in service. Limestone is the most encountered natural aggregate source due to the geological formation in the country, and in most of those quarries, limestone is revealed, processed, and transferred to use for different engineering

purposes including concrete manufacturing and pavement construction (Gökalp et al. 2018). When transportation costs are affordable, basalt sources are preferred, especially for pavement constructions, because of their superior physical and mechanical properties. On the other hand, Turkey is one of the biggest steel manufacturing countries, with more than 33 million tons of annual

Table 2. Aggregate spreading rate

Chip sizes (mm)	ALD (mm)	ASR for natural aggregates (mL)		ASR for slags (mL)
		Calculated	Used	Used
8–10	9	710.53	720.0	800.0
10–12	11	888.16	900.0	1,000.0

© ASCE 04020040-3 J. Mater. Civ. Eng.

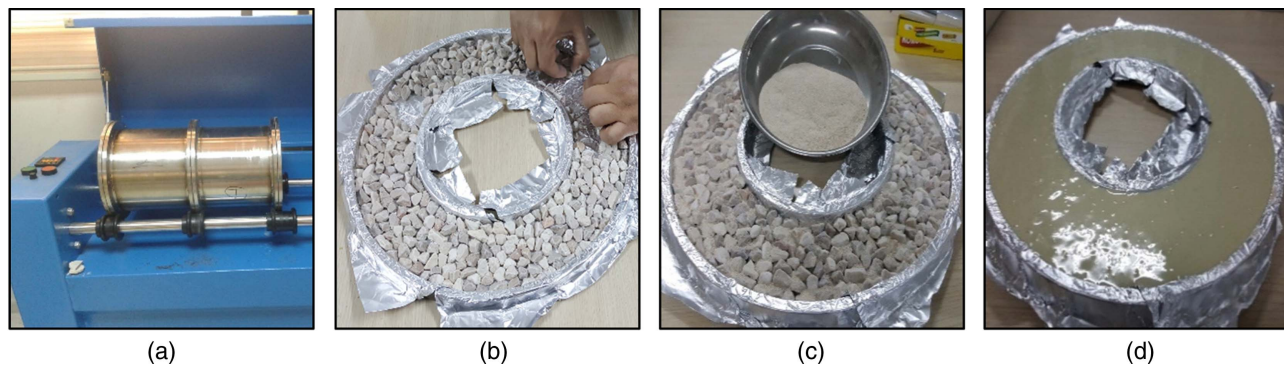J. Mater. Civ. Eng., 2020, 32(4): 04020040

Fig. 3. Production process of the chip seal samples: (a) polishing of aggregate with MD; (b) measuring the chips by volume; (c) filling the gap between chips; and (d) curing test samples.

production (WSA 2018). During the steel manufacturing process, 10%–15% of the total production is composed as slag and most of these by-products are deposited in storage areas.

This study aimed to investigate the effect of aggregate surface texture loss on the skid resistance of the pavement surface. To achieve it, chip seals (used as a surface layer in low-volume roads, and can be beneficial as a tool in maintaining and recovering skid resistance due to their cost-effective, less labor-intensive, and fast-built properties) were produced in the laboratory using different aggregate types (limestone, basalt, river basin crushed aggregate, and steel and ferrochromium slags) by different chip sizes (8–10 and 10–12 mm) and at three different polishing levels. Physical and chemical properties of aggregates were identified by a series of tests. Visual inspection of aggregates at each polishing level was done by SEM and OPM. OFM was used for the macro-texture evaluation of chip seal samples, while DFT and BPT were utilized for the assessment of skid resistance. IFI parameters, F(60) and Sp, were also determined for further assessment in case of different speeds and testers.

Production Process of Chip Seal Samples

Materials

Five types of aggregate, including natural (limestone, basalt, river basin crushed aggregate) and metallurgical by-products (steel and ferrochromium slags) were utilized in the scope of this study. Physical and mechanical properties of the aggregates are determined according to the related standards [EN 1097-1 (CEN 2011), EN 1097-2 (CEN 2010), EN 1097-8 (CEN 2009a), EN 1367-2 (CEN 2009b), EN 1097-6 (CEN 2013), EN 933 (CEN 2014), and ASTM C 142 (ASTM 2017)] and the results are presented in Table 1.

It can be seen from Table 1 that slags have better resistance to polishing, abrasion, fragmentation, and weathering, as compared with the natural aggregates. However, unit weight and water absorption values are found to be higher for slags.

The hardness, durability, soundness, and toughness of aggregates surely depend on not only physical properties but also chemical characteristics (Kazi and Al-Mansour 1980; Magnoni et al. 2016; Yildirim and Prezzi 2011), therefore chemical elements and mineral compositions of aggregates were determined by X-ray fluorescence (XRF) and X-ray diffraction (XRD) analysis, and the results are presented in Figs. 1 and 2, respectively.

As expected, calcium oxide and silicon dioxide were the main components of limestone and basalt, respectively. Both of these

elements were observed in the river basin crushed aggregate, which is a sedimentary rock. In addition to calcium oxide and silicon dioxide elements, ferric oxide was found as another chemical component of electric arc furnace (EAF) steel slag. Finally, silicon dioxide, magnesia, and alumina elements were observed in ferrochrome slags. The chemical and mineral components of the materials vary based on their geological formation or manufacturing process. It is known that chemical components influence hardness, durability, soundness, and toughness properties of aggregates. To clarify, it can be said that higher calcium carbonate composition decreases the polishing resistance of aggregates. Silica cause an alkali-silica reaction or alkali-carbonate reaction, particularly in humid and warm climates, and magnesia leads to significant expansion and cracking in aggregates. Accordingly, these contents make aggregates vulnerable against weathering. Al_2O_3 and Fe_2O_3 are compositions that make the materials harder and tougher against external forces.

Aggregate Spreading Rate

The purpose of this study was to evaluate the effect of microtexture changes on the skid resistance; therefore, to avoid any misleading test results, aggregates must be used at standard size, shape, and spreading rates. To do so, aggregates were sieved and then flaky and elongated particles were removed to obtain single size and cubic particles (ASTM 2012b). A ring plate with 10 cm inner and 19 cm outer diameter was used to prepare chip seal samples. To fill the plate uniformly and identify a standard aggregate application amount for natural aggregates and by-products, an aggregate spreading rate (ASR) was determined according to the average least
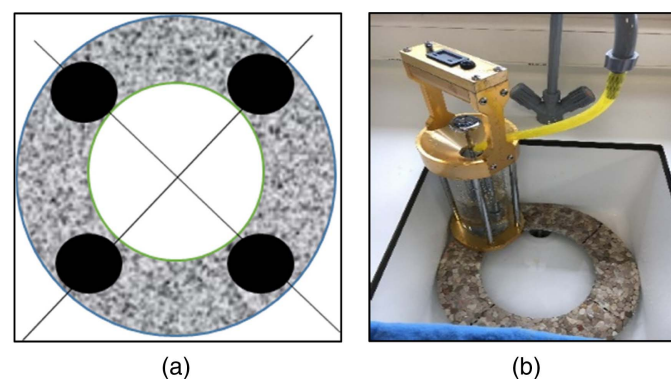

Fig. 4. OFM testing process on chip seal samples: (a) test points; and (b) application of the test.

Table 3. MTDs for chip seal samples at different polishing levels

Grain sizes (mm)	Polishing level	MTDs and StD (mm)									
		LS	StD	BS	StD	BLD	StD	EAF	StD	FER	StD
8–10	Unpolished	1.74	0.108	1.69	0.102	1.60	0.023	1.71	0.121	1.50	0.113
	1st polishing	1.59	0.243	1.42	0.069	1.39	0.065	1.62	0.261	1.39	0.067
	2nd polishing	1.34	0.094	1.43	0.230	1.29	0.097	1.47	0.093	1.40	0.043
10–12	Unpolished	2.09	0.273	1.78	0.065	1.76	0.109	2.14	0.192	1.63	0.115
	1st polishing	1.91	0.173	1.59	0.101	1.63	0.111	2.01	0.171	1.61	0.258
	2nd polishing	1.74	0.156	1.58	0.090	1.52	0.103	1.71	0.202	1.50	0.108

Note: LS = limestone; BS = basalt; BLD = river basin crushed aggregate; EAF = electric arc furnace steel slag; FER = ferrochromium slag; and StD = standard deviation.

dimension (ALD) [Eq. (1)]. ALD represents the expected chip seal thickness when the aggregates are oriented to lie on their flattest side (TNZ 2005). The calculation of ASR for aggregates is presented in Table 2. When measuring the ASR values in beakers, higher gaps were observed for slags because of their rough structure. Therefore, the ASR of slags was increased by 10%

$$ASR = \frac{950}{ALD} \qquad (1)$$

Aggregate Polishing Method

Polishing of aggregates was provided by utilizing the MD apparatus based on ASTM D6928 B gradation class (ASTM 2012e). The polishing levels were identified according to revolution numbers (RNs) of MD test. RNs were selected as 10,500 and 31,500 for the 1st and 2nd polishing levels, respectively, the same as had been applied in other studies (Lane et al. 2011; Uz and Gökalp 2017b; Wang et al. 2015a; Xue et al. 2010).

Chip Seal Production

Chip seal production process was also standardized to avoid any misleading results at texture and skid resistance measurements. This standard production process is summarized in the following paragraph and images taken during the work are given in Fig. 3.

Initially, aggregates were sieved for the MD test associated with related ASTM standard, then aggregates were polished using the test apparatus at different RNs. After the polishing process, one more sieve analysis was conducted to obtain 8–10 mm and 10–12 mm single size chips [Fig. 3(a)]. The next step was measuring aggregates in a volumetric beaker to spread over the aluminum foil paper covered plate [Fig. 3(b)]. Subsequently, 0.300–0.600 mm limestone powder was poured on the surface to fill two-thirds of the voids in-depth to ensure a certain macrotexture for each sample [Fig. 3(c)]. The resin was used for an adhesive purpose. After hardening, the sample was removed from the plate and allowed to cure for approximately 24 h [Fig. 3(d)].

Test Program

Within this study, mean texture depth (MTD) of the produced chip seal samples was determined with OFM. The assessment of skid resistance performance was done with DFT and BPT. Also, IFI was calculated through its two parameters, F(60) and Sp. Finally, SEM and OPM images taken from each sample at each polishing level were presented for making a visual inspection.

Outflow Meter Test

In this study, ASTM E2380, which identifies the operating principle of the outflow meter test (ASTM 2012c) was followed. The

test was implemented on each sample at four points with three repetitions. The arithmetic mean of the time gathered by outflow meter timer was recorded, and MTDs were calculated using Eq. (2). A sketch and photos of the testing process are presented in Fig. 4

$$MTD(mm) = (3.114/OFT) + 0.636 \qquad (2)$$

DFT Method

The test was performed on each sample according to ASTM E1911. The application procedure of the test is presented in detail by Rado and Kane (2014). However, it is worth indicating the significant properties of the device and the method. The measurement units of the device can be controlled by a connected laptop computer and the data can be displayed on the screen and stored on a disk. The results are reported as friction coefficient (μ) at different speeds ranging from 10 to 80 km/h, and change of friction coefficient of the surface by speed can be displayed on a graph (ASTM 2009; Saito et al. 1996).
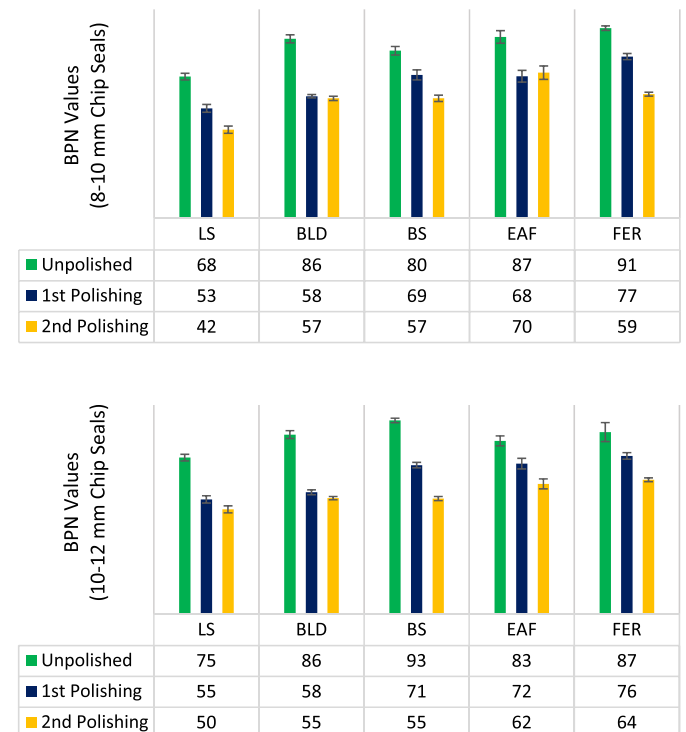

BPN Values (8-10 mm Chip Seals)	LS	BLD	BS	EAF	FER
Unpolished	68	86	80	87	91
1st Polishing	53	58	69	68	77
2nd Polishing	42	57	57	70	59

BPN Values (10-12 mm Chip Seals)	LS	BLD	BS	EAF	FER
Unpolished	75	86	93	83	87
1st Polishing	55	58	71	72	76
2nd Polishing	50	55	55	62	64

Fig. 5. BPT results of chip seals with different grain sizes at each polishing level. LS = limestone; BS = basalt; BLD = river basin crushed aggregate; EAF = electric arc furnace steel slag; and FER = ferrochromium slag.

© ASCE   04020040-5   J. Mater. Civ. Eng.

J. Mater. Civ. Eng., 2020, 32(4): 04020040

BPT Method

BPT is a static type tester with rubber pads. With this test, researchers can get an idea about the frictional property of pavement surfaces both in the field and in the laboratory. BPT provides a low-speed (approximately 10 km/h) skid resistance measurement. Within this study, this test was conducted according to ASTM E303 and the results were reported in terms of British pendulum numbers (BPNs). The following briefly describes the method used. The first step is calibration of the pendulum arm for zero value. The test operator then adjusts the touch length of the rubber pads by leveling the height of the tester. Before test application, the surface and the slider must be wetted to simulate the worst situation for

the skidding. Finally, the pendulum arm is released and the drag-pointer reading is taken. These steps are repeated at least four times, and the average value is reported as the BPN value of the surface (ASTM 2012d).

International Friction Index

IFI is used throughout the world as a common reference scale for quantifying the pavement skid resistance. IFI consists of friction number, F(s), and speed constant, Sp (ASTM 2012a). It is possible to calculate the coefficient of friction F(s) at any speed with different test methods such as BPT, DFT, and LWSRT (Pereira et al. 2018). The surface means texture depth is used to calculate speed
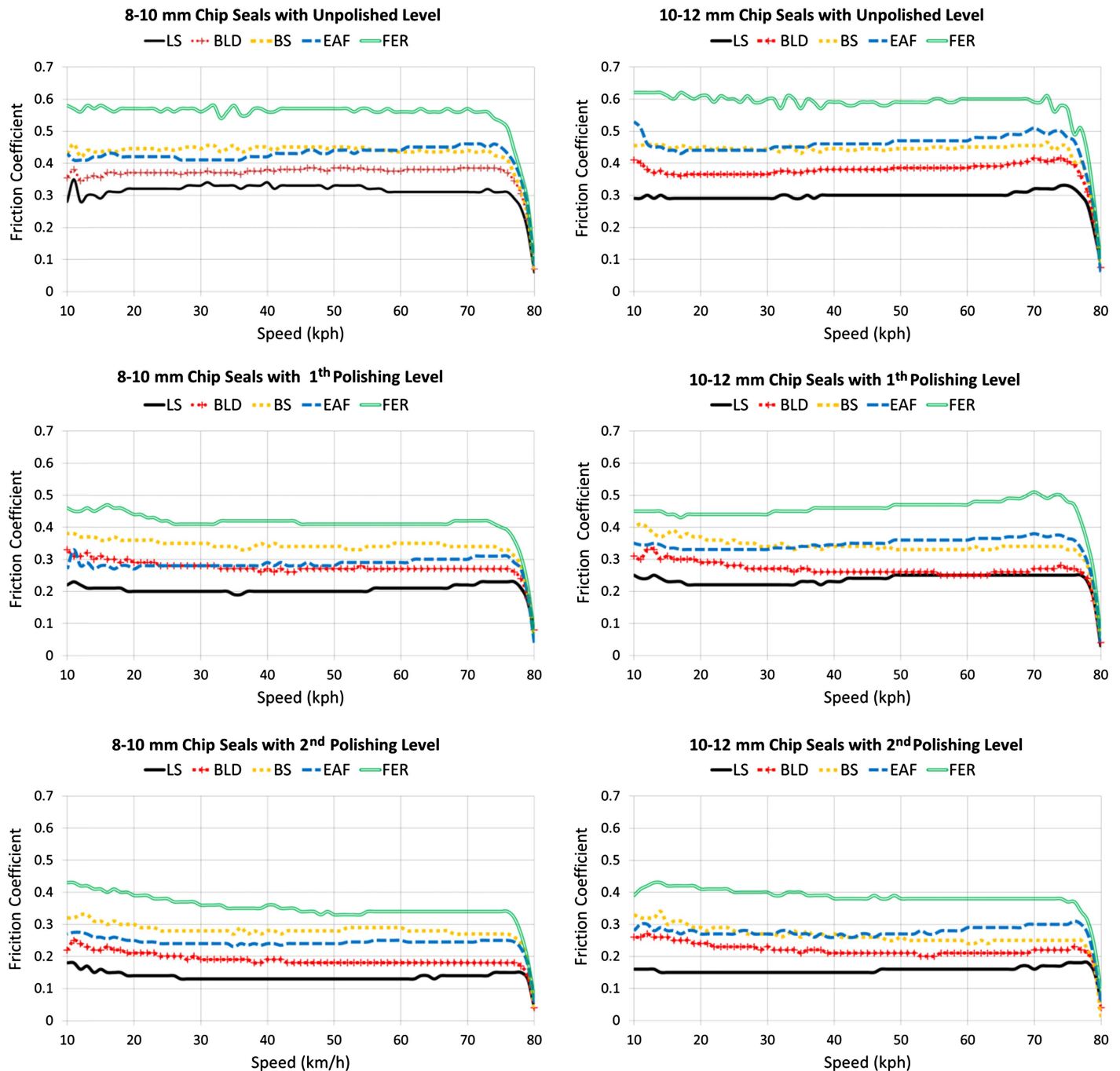

Fig. 6. DFT results of chip seals with different grain sizes at each polishing level. LS = limestone; BS = basalt; BLD = river basin crushed aggregate; EAF = electric arc furnace steel slag; and FER = ferrochromium slag.

© ASCE 04020040-6 J. Mater. Civ. Eng.

J. Mater. Civ. Eng., 2020, 32(4): 04020040

constant. In the scope of this study, MTDs were obtained by out-flow meter test methods, whereas BPT and DFT test results were used to calculate the friction numbers.

- Calculating Sp values using the MTD by using Eq. (3)

$$Sp = -11.6 + 113.6 \times MTD \qquad (3)$$

- Converting friction measurement FR(s) at slip speed S to friction at 60 km/h for the selected devices using Eq. (4)

$$FR(60) = FR(s) \times e^{\frac{(S-60)}{Sp}} \qquad (4)$$

- The general formulation of IFI, F(60), is given in Eq. (5), where a and b are the constants. The specified models for BPT and DFT devices are given in Eqs. (6) and (7), respectively

$$F(60) = a + b \times FR(60) \qquad (5)$$

$$F(60) = 0.056 + 0.008 \times BPN \times e^{\frac{(S-60)}{Sp}} \qquad (6)$$

$$F(60) = 0.081 + 0.735 \times DFT \times e^{\frac{(S-60)}{Sp}} \qquad (7)$$

Visual Inspection of Aggregate Polishing

SEM and OPM were utilized to monitor the surface of aggregates to make a visual assessment of the microtexture at each polishing level. It is a versatile tool that makes a microlevel assessment of any material. The model of the SEM was SNE-4500M, and could provide high-quality images and easily magnify up to $100.000\times$ with 5 and 10 nm resolution for secondary electrons (SE) and back-scattered electrons (BSE) images, respectively. The SEM sample processing was done according to the vacuum-dried method within the current study. Randomly selected 8–10 mm chips for each aggregate type and polishing level were monitored with OPM and SEM to make a visual assessment at both macrolevel and micro-level, respectively. In addition, OPM was utilized for comparison of aggregates polished with MD and polish stone value (PSV) tests.

Results and Discussion

Texture Measurements

MTDs were gathered by OFM test method for all chip seal samples with different chip sizes and the results are presented in Table 3, including standard deviations.

Calculated standard deviations given in Table 3 for each sample demonstrated that the sample preparation process was done almost uniformly. Moreover, it can be seen that samples with bigger chip sizes had higher MTDs values.

Skid Resistance Measurements

BPT is a kind of operator-dependent device. To eliminate the effect of the operator, the test for each sample was performed by a single operator. The skid resistance results of chip seals manufactured with different grain size and at each polishing level are given in Figs. 5 and 6 for BPN and DFT, respectively. To show the decrease in skid resistance by increasing polishing duration, Fig. 7 was created for DFT results at 60 km/h.

The following can be implied in light of the data presented in Figs. 5–7. The tendency of the development of friction coeffi-cients decreased with the increase in polishing levels. The results of BPT exhibited the same profile as DFT results, a situation that was expected. Due to their texture, the highest skid resistance
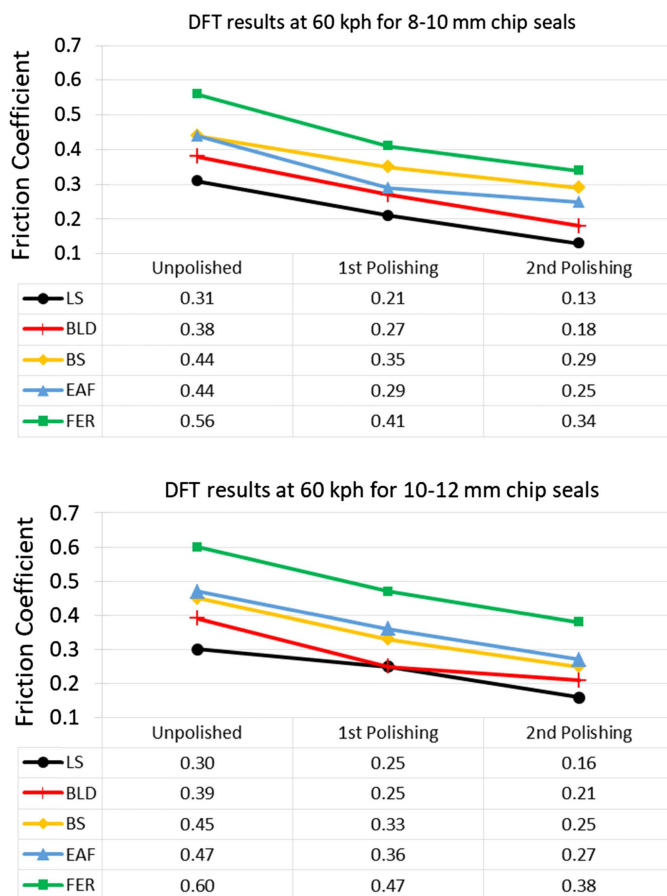

DFT results at 60 kph for 8-10 mm chip seals

	Unpolished	1st Polishing	2nd Polishing
LS	0.31	0.21	0.13
BLD	0.38	0.27	0.18
BS	0.44	0.35	0.29
EAF	0.44	0.29	0.25
FER	0.56	0.41	0.34

DFT results at 60 kph for 10-12 mm chip seals

	Unpolished	1st Polishing	2nd Polishing
LS	0.30	0.25	0.16
BLD	0.39	0.25	0.21
BS	0.45	0.33	0.25
EAF	0.47	0.36	0.27
FER	0.60	0.47	0.38

Fig. 7. DFT results at 60 km/h.

Table 4. Sp values

Grain size (mm)	Polishing level	Sp				
		LS	BS	BLD	EAF	FER
8–10	Unpolished	186.1	180.4	170.2	182.7	158.8
	1st polishing	169.0	149.7	146.3	172.4	146.3
	2nd polishing	140.6	150.8	134.9	155.4	147.4
10–12	Unpolished	225.8	190.6	188.3	231.5	173.6
	1st polishing	205.4	169.0	173.6	216.7	171.3
	2nd polishing	186.1	167.9	161.1	182.7	158.8

Note: LS = limestone; BS = basalt; BLD = river basin crushed aggregate; EAF = electric arc furnace steel slag; and FER = ferrochromium slag.

performances were observed in slags, whereas the limestone exhibited the lowest performance among all the aggregates for all polishing levels. In general, the friction coefficients of 8–10 mm and 10–12 mm chip seal samples were much more close to each other at each polishing level.

IFI Results

Sp and F(60) values were calculated based on the obtained MTDs, BPNs, and DFT friction coefficient results. Tables 4 and 5 show the results based on aggregate parameters including the type, size, and polishing level for the mentioned speed.

Sp values presented in Table 4 decrease as the polishing level increases. The data in Table 5 indicated that lower friction coeffi-cients were observed at higher polishing levels. Also, F(60) values calculated by BPNs exhibited a similar tendency than that calcu-lated by the friction coefficient gathered by DFT.

Table 5. F(60) values based on the results of DFT and BPT

Speed (km/h)	Grain size (mm)	Polishing levels	F(60)_{DFT}					F(60)_{BPT}				
			LS	BLD	BS	EAF	FER	LS	BLD	BS	EAF	FER
60	8–10	Unpolished	0.308	0.359	0.403	0.403	0.491	0.598	0.743	0.698	0.750	0.784
		1st polishing	0.235	0.279	0.337	0.293	0.381	0.477	0.523	0.605	0.600	0.675
		2nd polishing	0.176	0.213	0.293	0.264	0.330	0.395	0.515	0.515	0.614	0.531
	10–12	Unpolished	0.301	0.366	0.410	0.425	0.520	0.654	0.742	0.797	0.718	0.752
		1st polishing	0.264	0.264	0.323	0.345	0.425	0.494	0.522	0.626	0.631	0.661
		2nd polishing	0.198	0.235	0.264	0.279	0.359	0.456	0.499	0.498	0.554	0.570

Note: LS = limestone; BS = basalt; BLD = river basin crushed aggregate; EAF = electric arc furnace steel slag; and FER = ferrochromium slag.
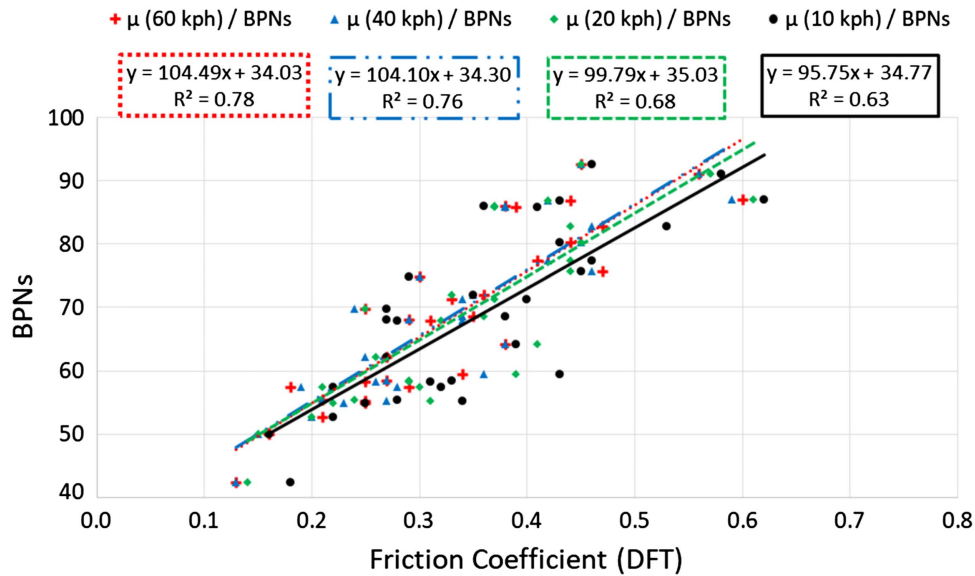
Fig. 8. Relationship between BPT and DFT results.

Correlational Analysis

To figure out any relationships between DFT and BPT methods, the test results for different speeds (10, 20, 40, and 60 km/h) are presented in Fig. 8.

Since BPT operates at low speed, a higher correlation had been expected to be achieved at low speeds. However, lower root square value (0.63) was determined at the lowest speed, while the higher correlations (0.78) were found at the highest speed. The reason for this finding might be the pavement type, different working and operating principles of devices, and the materials used. With this conclusion, it may be worth it to highlight that the results of BPT can be used to estimate the friction coefficient of a surface, especially chip sealed surface at higher speeds.

To make a further analysis, Fig. 9 was created to compare IFI F (60) values that were calculated based on both friction coefficient and BPNs. In Fig. 9, similar to the relationship between BPN and friction coefficient, a good correlation was observed between F(60) values.

SEM and OPM Images

To evaluate the microtexture of aggregate at the same level, 90× magnification factor was used in SEM analysis of 8–10 mm chips. However, only limestone's microtexture can be captured at 90× magnification level. Focusing on the surface at this level became impossible for other aggregates, especially for slags, because of

their rough (irregular) surface. SEM images for each aggregate at different polishing levels are given in Fig. 10.

The SEM images in Fig. 10 show that the initial (unpolished level) microtexture of each aggregate type was different, and the surface of each one was becoming smoother with the increasing polishing levels. The images of the limestone show that its surface was smoother than the other two natural ones. On the other hand, slags had much more porous structure even at the highest polishing level. It can be seen from the SEM images that the porous structure
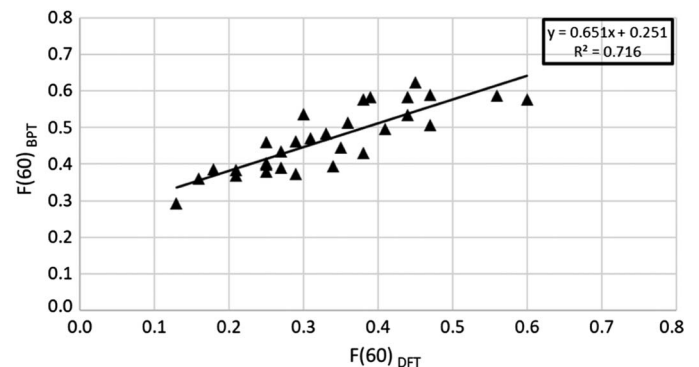
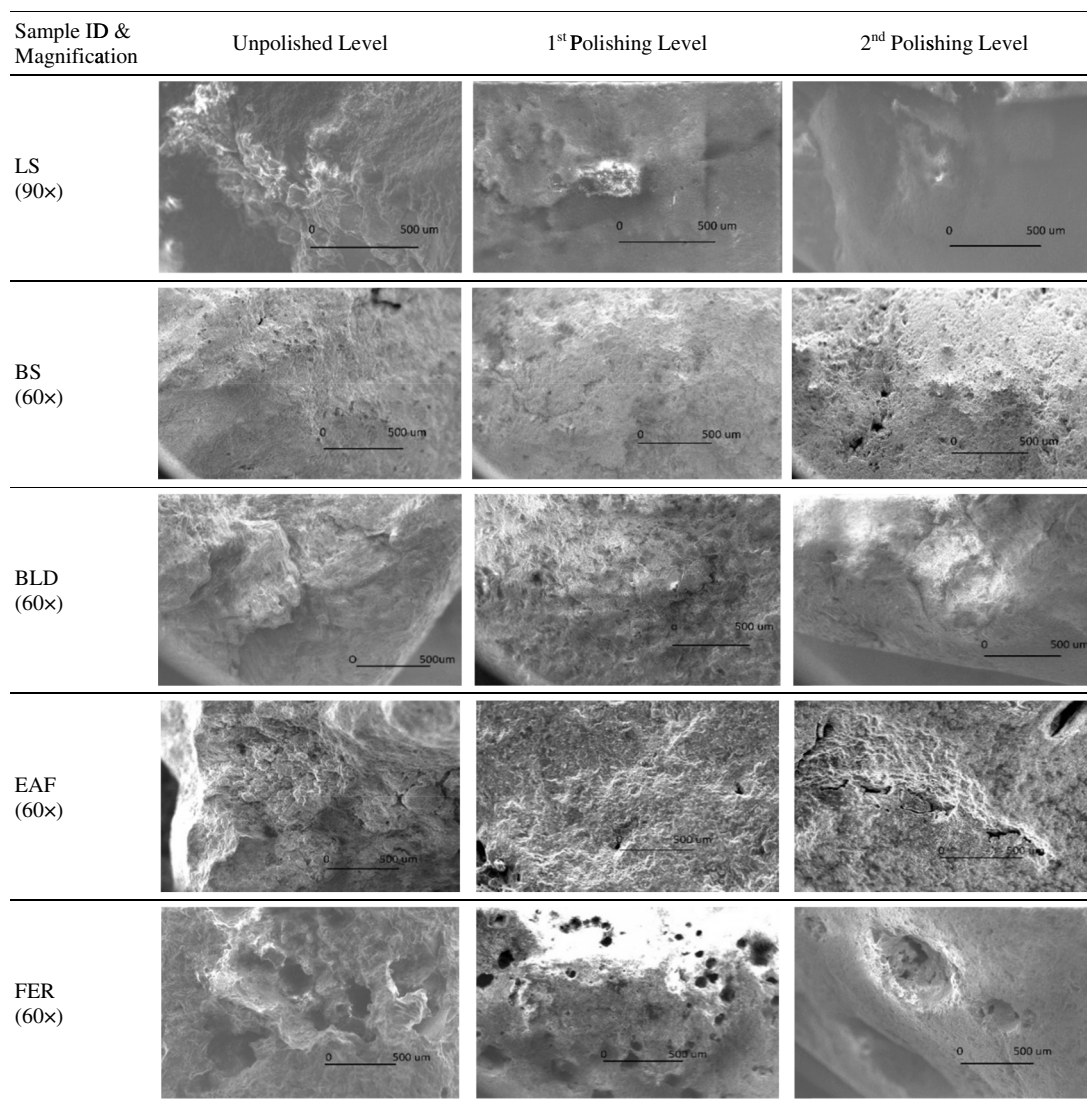**Fig. 9.** Relationship between F(60) values based on BPT and DFT results.

Sample ID & Magnification	Unpolished Level	1st Polishing Level	2nd Polishing Level
LS (90×)			
BS (60×)			
BLD (60×)			
EAF (60×)			
FER (60×)			

Fig. 10. SEM images of aggregate at each polishing level. LS = limestone; BS = basalt; BLD = river basin crushed aggregate; EAF = electric arc furnace steel slag; and FER = ferrochromium slag.

of slags at the second polishing level is almost like the unpolished level of natural aggregates.

Additionally, OPM images were taken from the first and second polishing levels of chip seals and PSV test samples (Fig. 11) for comparison of different methods and to show the feasibility of MD apparatus to assess polishing resistances of samples.

Summary and Conclusions

In this paper, chip seal samples were produced at the laboratory in a ring plate with different aggregate types, grain sizes, and polishing levels. The polishing levels were provided using certain drum revolutions of the MD apparatus following the ASTM standard. DFT, BPT, and OFM tests were conducted to determine the skid resistance and texture properties of each sample. IFI parameter for 60 km/h speed was determined using the two skid resistance testers' results. SEM and OPM images were also taken to make clear sense of the tendency of loss in the microtexture of aggregate utilizing the MD method. Based on the findings of this investigation, the following conclusions can be highlighted:

- In the sense of aggregate type, slags have superior properties compared to natural aggregates.
- Skid resistance of chip seals decreased as the polishing level increased for each aggregate type and chip size.
- The chip seals produced with slags showed better skid resistance performance compared to the natural aggregates at each polishing level.
- Slag is considered a high polishing resistant material that can assist in the production of long-lasting surface coatings.
- Good correlations were established between the results of BPT and DFT. Interestingly, lower root square value was observed at lower speeds of DFT and the studied pavement type could be the reason. In addition, a good relationship was found between F(60) values gathered with DFT and BPT results.
- SEM and OPM images made clear sense about the microtexture of aggregates and its loss with the polishing process.
- The findings of this study show that the MD test method (modified version in extent) is an available method to polish aggregate as well as the PSV test method. The authors believe that MD apparatus can be an alternative, simple, and cost- and time-effective tool for evaluating the polishing resistance of aggregates.
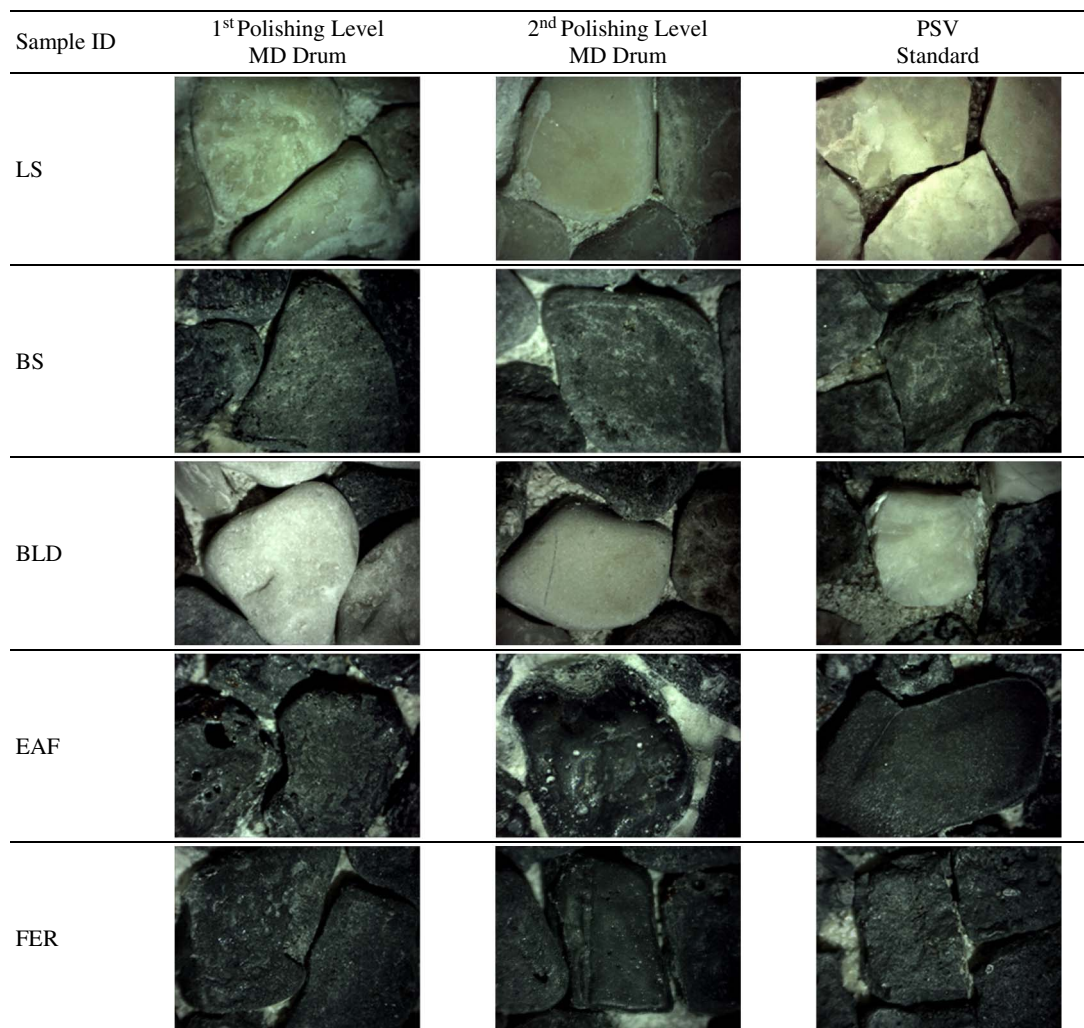
© ASCE 04020040-9 J. Mater. Civ. Eng.

J. Mater. Civ. Eng., 2020, 32(4): 04020040

Fig. 11. OPM images of aggregates based on different polishing methods. LS = limestone; BS = basalt; BLD = river basin crushed aggregate; EAF = electric arc furnace steel slag; and FER = ferrochromium slag.

Data Availability Statement

All data, models, and code generated or used during the study appear in the published article.

Acknowledgments

References

Ansari, S., F. Akhdar, M. Mandoorah, and K. Moutaery. 2000. "Causes and effects of road traffic accidents in Saudi Arabia." *Public Health* 114 (1): 37–39. https://doi.org/10.1016/S0033-3506(00)00306-1.

ASTM. 2009. *Standard test method for measuring paved surface frictional properties using the dynamic friction tester*. ASTM E1911. West Conshohocken, PA: ASTM.

ASTM. 2012a. *Standard practice for calculating international friction index of pavement surface*. ASTM E1960. West Conshohocken, PA: ASTM.

ASTM. 2012b. *Standard test method for flat particles, elongated particles, or flat and elongated particles in coarse aggregate*. ASTM D4791. West Conshohocken, PA: ASTM.

ASTM. 2012c. *Standard test method for measuring pavement texture drainage using an outflow meter*. ASTM E2380. West Conshohocken, PA: ASTM.

ASTM. 2012d. *Standard test method for measuring surface frictional properties using the british pendulum tester*. ASTM E303. West Conshohocken, PA: ASTM.

ASTM. 2012e. *Standard test method for resistance of coarse aggregate to degradation by abrasion in the micro-deval apparatus*. ASTM 6928-10. West Conshohocken, PA: ASTM.

ASTM. 2017. *Standard test method for clay lumps and friable particles in aggregates*. ASTM C142/C142M-17. West Conshohocken, PA: ASTM.

Bessa, I. S., V. T. F. Castelo Branco, and J. B. Soares. 2014. "Evaluation of polishing and degradation resistance of natural aggregates and steel slag using the aggregate image measurement system." *Road Mater. Pavement Des.* 15 (2): 385–405. https://doi.org/10.1080/14680629.2014.883323.

Black, G. W., Jr., and L. E. Jackson. 2000. "Pavement surface water phenomena and traffic safety." *ITE J.* 70 (2): 32–37.

© ASCE 04020040-10 J. Mater. Civ. Eng.

J. Mater. Civ. Eng., 2020, 32(4): 04020040

Cafiso, S., and S. Taormina. 2007. "Texture analysis of aggregates for wearing courses in asphalt pavements." *Int. J. Pavement Eng.* 8 (1): 45–54. https://doi.org/10.1080/10298430600898307.

CEN (European Committee for Standardization). 2009a. *Tests for mechanical and physical properties of aggregates determination of the polished stone value*. BS EN 1097-8. Brussels, Belgium: CEN.

CEN (European Committee for Standardization). 2009b. *Tests for thermal and weathering properties of aggregates Magnesium sulfate test*. BS EN 1367-2. Brussels, Belgium: CEN.

CEN (European Committee for Standardization). 2010. *Tests for mechanical and physical properties of aggregates—Methods for the determination of resistance to fragmentation*. BS EN 1097-2. Brussels, Belgium: CEN.

CEN (European Committee for Standardization). 2011. *Tests for mechanical and physical properties of aggregates—Determination of the resistance to wear (micro-Deval)*. BS EN 1097-1. Brussels, Belgium: CEN.

CEN (European Committee for Standardization). 2013. *Tests for mechanical and physical properties of aggregates—Determination of particle density and water absorption*. BS EN 1097-6. Brussels, Belgium: CEN.

CEN (European Committee for Standardization). 2014. *Tests for geometrical properties of aggregates—Assessment of surface characteristics. Flow coefficient of aggregates*. BS EN 933-6. Brussels, Belgium: CEN.

Chaurand, P., J. Rose, V. Briois, L. Olivi, J.-L. Hazemann, O. Proux, J. Domas, and J.-Y. Bottero. 2007. "Environmental impacts of steel slag reused in road construction: A crystallographic and molecular (XANES) approach." *J. Hazard. Mater.* 139 (3): 537–542. https://doi.org/10.1016/j.jhazmat.2006.02.060.

Cossale, G., R. Elliott, and I. Widyatmoko. 2013. "The importance of road surface texture in active road safety design and assessment." In *Proc., Int. Conf. on Road Safety and Simulation RSS*. Amsterdam, Netherlands: National Safety Council and Elsevier.

Crouch, L., and W. Goodwin. 1995. *Identification of aggregates for tennessee bituminous surface courses*. Phase II Final Rep. No. TN-RES1056. Nashville, Tennessee: Tennessee Dept. of Transportation.

Do, M.-T., and V. Cerezo. 2015. "Road surface texture and skid resistance." *Surf. Topogr.: Metrol. Prop.* 3 (4): 043001. https://doi.org/10.1088/2051-672X/3/4/043001.

Do, M.-T., Z.-D. Tang, M. Kane, and F. De Larrard. 2009. "Evolution of road surface skid resistance and texture due to polishing." *Wear* 266 (5): 574–577. https://doi.org/10.1016/j.wear.2008.04.060.

El-Assaly, A., and R. Ellis. 2001. "Evaluation of recycling waste materials and by-products in highway construction." *Int. J. Sustainable Dev. World Ecol.* 8 (4): 299–308. https://doi.org/10.1080/13504500109470088.

Flintsch, G., E. de Leon, K. McGhee, and I. AI-Qadi. 2003. "Pavement Surface Macrotexture Measurement and Applications." *Transp. Res. Rec.* 1860 (1): 168–177. https://doi.org/10.3141/1860-19.

Friel, S., and D. Woodward. 2013. "Predicting the development of asphalt surfacing properties in Ireland." In *Proc., Airfield and Highway Pavement 2013: Sustainable and Efficient Pavements*, 829–840. Reston, VA: ASCE.

Gökalp, İ., and V. E. Uz. 2017. "A brief overview on pavement skid resistance and measurement methods." In *Proc., Int. Advanced Researches and Engineering Congress*, 1861–1866. Osmaniye, Turkey: Osmaniye Korkut Ata Univ.

Gökalp, İ., V. E. Uz, M. Saltan, and E. Tutumluer. 2018. "Technical and environmental evaluation of metallurgical slags as aggregate for sustainable pavement layer applications." *Transp. Geotech.* 14 (Mar): 61–69. https://doi.org/10.1016/j.trgeo.2017.10.003.

Kane, M., I. Artamendi, and T. Scarpas. 2013. "Long-term skid resistance of asphalt surfacings: Correlation between Wehner–Schulze friction values and the mineralogical composition of the aggregates." *Wear* 303 (1): 235–243. https://doi.org/10.1016/j.wear.2013.03.022.

Karlaftis, M. G., and I. Golias. 2002. "Effects of road geometry and traffic volumes on rural roadway accident rates." *Accid. Anal. Prev.* 34 (3): 357–365. https://doi.org/10.1016/S0001-4575(01)00033-1.

Kazi, A., and Z. R. Al-Mansour. 1980. "Influence of geological factors on abrasion and soundness characteristics of aggregates." *Eng. Geol.* 15 (3–4): 195–203. https://doi.org/10.1016/0013-7952(80)90034-4.

Kehagia, F. 2009. "Skid resistance performance of asphalt wearing courses with electric arc furnace slag aggregates." *Waste Manage. Res.* 27 (3): 288–294. https://doi.org/10.1177/0734242X08092025.

Kogbara, R. B., E. A. Masad, E. Kassem, and A. Scarpas. 2018. "Skid resistance characteristics of asphalt pavements in hot climates." *J. Transp. Eng., Part B: Pavements* 144 (2): 04018015. https://doi.org/10.1061/JPEODX.0000046.

Krayushkina, K., O. Prentkovskis, A. Bieliatynskyi, and R. Junevičius. 2012. "Use of steel slags in automobile road construction." *Transport* 27 (2): 129–137. https://doi.org/10.3846/16484142.2012.690093.

Kua, H. W. 2015. "Integrated policies to promote sustainable use of steel slag for construction-a consequential life cycle embodied energy and greenhouse gas emission perspective." *Energy Build.* 101 (Aug): 133–143. https://doi.org/10.1016/j.enbuild.2015.04.036.

Lane, D., C. Druta, L. Wang, and W. Xue. 2011. "Modified microdeval procedure for evaluating the polishing tendency of coarse aggregates." *Transp. Res. Rec.* 2232 (1): 34–43. https://doi.org/10.3141/2232-04.

Magnoni, M., F. Giustozzi, E. Toraldo, and M. Crispino. 2016. "Evaluation of the effect of aggregates mineralogy and geometry on asphalt mixture friction." *J. Civ. Environ. Eng.* 6 (223): 2.

Mahmoud, E., and E. Masad. 2007. "Experimental methods for the evaluation of aggregate resistance to polishing, abrasion, and breakage." *J. Mater. Civ. Eng.* 19 (11): 977–985. https://doi.org/10.1061/(ASCE)0899-1561(2007)19:11(977).

Mataei, B., H. Zakeri, M. Zahedi, and F. M. Nejad. 2016. "Pavement friction and skid resistance measurement methods: A literature review." *Open J. Civ. Eng.* 6 (4): 537. https://doi.org/10.4236/ojce.2016.64046.

Mayora, J. M. P., and R. J. Piña. 2009. "An assessment of the skid resistance effect on traffic safety under wet-pavement conditions." *Accid. Anal. Prev.* 41 (4): 881–886. https://doi.org/10.1016/j.aap.2009.05.004.

McLean, J. 1995. "The relationship between pavement conditions and road safety." In *Proc., Load-Pavement Interaction Workshop, 1995*. Vermont South, Australia: Australian Road Research Board.

Nataadmadja, A. D., D. J. Wilson, S. B. Costello, and M. T. Do. 2015. "Correlating laboratory test methodologies to measure skid resistance of pavement surfaces." *Transp. Res. Rec.* 2506 (1): 107–115. https://doi.org/10.3141/2506-12.

Ortiz, E. M., and E. Mahmoud. 2014. "Experimental procedure for evaluation of coarse aggregate polishing resistance." *Transp. Geotech.* 1 (3): 106–118. https://doi.org/10.1016/j.trgeo.2014.06.001.

Ossa, A., J. García, and E. Botero. 2016. "Use of recycled construction and demolition waste (CDW) aggregates: A sustainable alternative for the pavement construction industry." *J. Cleaner Prod.* 135 (Nov): 379–386. https://doi.org/10.1016/j.jclepro.2016.06.088.

Pereira, P. A., J. C. Pais, G. Trichês, and L. P. Fontes. 2018. "Skid resistance and texture of compacted asphalt mixes evaluated from the IFI in laboratory preparation." In *Proc., 4th Eurasphalt and Eurobitume Congress*, 1–14. Brussels, Belgium: European Asphalt Pavement Association.

PIARC (World Road Association). 1987. "Report of the committee on surface characteristics." In *Proc., XVIII World Road Congress*. La Défense cedex, France: World Road Association.

Plank, R. 2008. "The principles of sustainable construction." *IES J. Part A: Civ. Struct. Eng.* 1 (4): 301–307. https://doi.org/10.1080/19373260802404482.

Praticò, F., and R. Vaiana. 2015. "A study on the relationship between mean texture depth and mean profile depth of asphalt pavements." *Constr. Build. Mater.* 101 (Dec): 72–79. https://doi.org/10.1016/j.conbuildmat.2015.10.021.

Prezzi, M., P. Bandini, J. A. H. Carraro, and P. J. Monteiro. 2011. "Use of recyclable materials in sustainable civil engineering applications." *Adv. Civ. Eng.* 2011: 2. https://doi.org/10.1155/2011/896016.

Rado, Z., and M. Kane. 2014. "An initial attempt to develop an empirical relation between texture and pavement friction using the HHT approach." *Wear* 309 (1–2): 233–246. https://doi.org/10.1016/j.wear.2013.11.015.

Saito, K., T. Horiguchi, A. Kasahara, H. Abe, and J. Henry. 1996. "Development of portable tester for measuring skid resistance and its speed

© ASCE   04020040-11   J. Mater. Civ. Eng.

J. Mater. Civ. Eng., 2020, 32(4): 04020040

dependency on pavement surfaces." *Transp. Res. Rec.* 1536 (1): 45–51. https://doi.org/10.1177/0361198196153600107.

Sarsam, S., and H. Al Shareef. 2015. "Assessment of texture and skid variables at pavement surface." *Appl. Res. J.* 1 (8): 422–432.

Sengoz, B., A. Topal, and S. Tanyel. 2012. "Comparison of pavement surface texture determination by sand patch test and 3D laser scanning." *Period. Polytech. Civ. Eng.* 56 (1): 73. https://doi.org/10.3311/pp.ci.2012-1.08.

TNZ (Transit New Zealand). 2005. "Road controling authorties and roading New Zeland 2005." In *Chipsealing in New Zealand*. Wellington, New Zealand: TNZ.

TUIK (Turkish Statistical Institute). 2017. "Road traffic accident statistics for Turkey, 2016." Accessed June 21, 2017. http://www.turkstat.gov.tr/PreHaberBultenleri.do?id=24606.

Uz, V. E., and İ. Gökalp. 2017a. "Comparative laboratory evaluation of macro texture depth of surface coatings with standard volumetric test methods." *Constr. Build. Mater.* 139 (May): 267–276. https://doi.org/10.1016/j.conbuildmat.2017.02.059.

Uz, V. E., and İ. Gökalp. 2017b. "The effect of aggregate type, size and polishing levels to skid resistance of chip seals." *Mater. Struct.* 50 (2): 126. https://doi.org/10.1617/s11527-017-0998-6.

Wang, D., X. Chen, C. Yin, M. Oeser, and B. Steinauer. 2013. "Influence of different polishing conditions on the skid resistance development of asphalt surface." *Wear* 308 (1): 71–78. https://doi.org/10.1016/j.wear.2013.09.013.

Wang, D., H. Wang, Y. Bu, C. Schulze, and M. Oeser. 2015a. "Evaluation of aggregate resistance to wear with micro-deval test in combination with aggregate imaging techniques." *Wear* 338–339 (Sep): 288–296. https://doi.org/10.1016/j.wear.2015.07.002.

Wang, D., X. Xie, M. Oeser, and B. Steinauer. 2015b. "Influence of the gritting material applied during the winter services on the asphalt surface performance." *Cold Reg. Sci. Technol.* 112 (Apr): 39–44. https://doi.org/10.1016/j.coldregions.2015.01.001.

Wang, H., D. Wang, P. Liu, J. Hu, C. Schulze, and M. Oeser. 2017. "Development of morphological properties of road surfacing aggregates during the polishing process." *Int. J. Pavement Eng.* 18 (4): 367–380. https://doi.org/10.1080/10298436.2015.1088153.

WSA (World Steel Association). 2018. *Steel statistical yearbook 2017*, 128. Brussels, Belgium: WSA.

Xirouchakis, D., and V. Manolakou. 2011. "Properties of an EAF slag produced in Greece, a construction material for sustainable growth." In *Proc., 5th Int. Conf. for Bituminous Mixtures and Pavements*, 1–10. Thessaloniki, Greece: Aristotle Univ.

Xue, W., C. Druta, L. Wang, and D. S. Lane. 2010 "Assessing the polishing characteristics of coarse aggregates using micro-deval and imaging system." In *Proc., GeoShanghai 2010 Int. Conf.*, 288–295. Reston, VA: ASCE.

Yildirim, I. Z., and M. Prezzi. 2011. "Chemical, mineralogical, and morphological properties of steel slag." *Adv. Civ. Eng.* 1–13. https://doi.org/10.1155/2011/463638.

Ziari, H., and M. M. Khabiri. 2007. "Preventive maintenance of flexible pavement and mechanical properties of steel slag asphalt." *J. Environ. Eng. Landscape Manage.* 15 (3): 188–192. https://doi.org/10.3846/16486897.2007.9636928.

© ASCE — 04020040-12 — J. Mater. Civ. Eng.

J. Mater. Civ. Eng., 2020, 32(4): 04020040